Performance of the Effective-characteristic-polynomial Π2 Method for Diatomic Molecules: Basis-set Dependencies and Vibrational Levels

Herbert H. H.Homeier and M. D. Neef
Email: herbert.homeier@na-net.ornl.gov
Institut für Physikalische und Theoretische Chemie
Universität Regensburg
D-93040 Regensburg, Germany

October 19, 1999

Abstract

The performance of the recently introduced Π2 method [1] is investigated for some diatomic molecules. For this end, ground state energies are calculated at the MP4 level for various basis sets of increasing size. With negligible extra effort, the Π2, F4, and [2/2] estimators are obtained, together with information on the reliability of the basic perturbation series [1]. The results are compared to more expensive CCSD(T) results. Also, electronic energy hypersurfaces are calculated at these levels. As a further possibility to test the performance of the method, vibrational frequencies and other spectroscopic constants of diatomic molecules are calculated by fitting different analytic functions to the hypersurfaces obtained by different methods and compared to experimental data.

[1] H. H. H. Homeier, Correlation energy estimators based on Møller-Plesset perturbation theory, *J. Mol. Struct. (Theochem)*, 366:161-171, 1996.
Category: Ab initio
Keywords: Correlation energy, Perturbation theory, Morse potential, Anharmonicity constant, Hypersurface, Spectroscopic constants

1 Introduction

Recently, methods have been discussed for the computation of correlation energy estimators based on Møller-Plesset (MP) perturbation theory that may also be regarded as accelerating the convergence of the MP series [1],[2],[3],[4],[5],[6],[7],[8],[9],[10]. In [8], some methods were discussed that are based on MP calculations of fourth order (MP4)[1]:

- The Feenberg energy of fourth order F4 [11],[12],[10],[8],
- The Padé approximant $[2/2]^2$, [13],[14],[15]
- The Π2 approximation that is computed as the zero of an effective characteristic polynomial [16],[17],[18],[19],[20],[21],[22],[23] of degree 2.

All these approximations are calculated from the terms of the MP series with negligible extra effort. Explicit formulas for these methods are given in Section 2. All the methods are size-extensive [8],[9]. Also, test calculations were reported in [8] for a rather large number of small molecules (BH, HF, CH_2, H_2O, NH_2, NH_3, CO, C_2H_2, O_3, CN) for which Full Configuration Interaction (FCI) or Coupled-Cluster (CC) including Single (S), Double (D) and Triple (T) excitations, i.e., CCSDT results are available, mainly for basis sets of double zeta (DZ) or DZ plus polarization (DZP) quality. It was shown that (for the treated cases) the Π2 method yields very good approximations for the energy if the values of F4, [2/2] and Π2 are sufficiently close together. If the latter criterion is satisfied, all three methods improve the MP4 values considerably. The above criterion to accept the result of the perturbation calculation is especially important since it is well-known that the quality of the MP results deteriorates for greater distances from the equilibrium geometry. Thus, the criterion allows to judge the quality of the MP series. The criterion will be further discussed in Section 2.

In the present contribution, we report further studies of the performance of the Π2 and also the F4 and [2/2] methods. In particular, the dependence on the choice of the basis sets is important for the application of the methods. We limit attention to diatomic systems. Also, we report some results concerning the quality of potential energy surfaces and the calculation of spectroscopic constants.

2 Methods

The ab initio MP4 and CCSD(T) calculations were done using the Gaussian 94 program package [24]. For all systems under study, we calculate properties of the lowest singlet state.

For the MP energy terms, we used

$$E2 = E(MP2) - E(SCF), \quad E3 = E(MP3) - E(MP2), \quad E4 = E(MP4SDTQ) - E(MP3). \tag{1}$$

Then, the F4 energy is given by

$$F4 = E(SCF) + \frac{E2^3\,(-E2 + 2\,E3 - E4)}{(-E2 + E3)^3} \tag{2}$$

and the [2/2] energy is[3]

constants three different approaches were examined. Two fits of a narrow region around the minimum by polynomials of degree 3 or 5 were used to calculate the five spectroscopic constants $\omega_e, \omega_e x_e, B_e, \alpha_e, D_e$, the equilibrium distance R_e, the force constant k_e and the minimum total electronic energy U_e. The third approach using a four parameter Morse potential as fit function yielded the two constants ω_e and $\omega_e x_e$.

The calculated spectroscopic constants arise from a second order approximation of the rovibrational energy as follows:

$$E_{tot}(v,J) = E_{vib}(v) + E_{rot}(v,J) \tag{7}$$

with

$$E_{vib}(v) = \omega_e(v+\frac{1}{2}) - \omega_e x_e(v+\frac{1}{2})^2 \tag{8}$$

and

$$E_{rot}(v,J) = B_v J(J+1) - D_v J^2(J+1)^2 \tag{9}$$

where

$$B_v = B_e - \alpha_e(v+\frac{1}{2}) \tag{10}$$

and

$$D_v = D_e + \beta_e(v+\frac{1}{2}). \tag{11}$$

The centrifugal distortion constant D_e should not be confused neither with the dissociation energy $\mathbf{D}_0$ nor the depth $\mathbf{D}_e$ of the potential at the minimum.

The Morse data were obtained by a least square fit of a Morse potential

$$U(R) = U_e + \mathbf{D}_e(1 - \exp(-\beta(R-R_e)))^2 \tag{12}$$

with fit parameters $U_e, \mathbf{D}_e, R_e, \beta$ to a suitable part of the calculated potential surface that was chosen according to the above criterion (6). A Fortran 77 program which used the NAG [26] routine E04FDF was used in the fitting procedure. We follow the spectroscopic praxis and choose cm^{-1} as unit for energies and frequencies in formulas and tables. The vibrational frequency ω_e and the first anharmonicity constant were then calculated from the parameters of the Morse potential using the formulas

$$\omega_e = \beta\sqrt{\frac{\hbar \mathbf{D}_e}{\pi c \mu}} \tag{13}$$

and

$$\omega_e x_e = \frac{\omega_e^2}{4\mathbf{D}_e} \tag{14}$$

where μ is the reduced mass of the diatomic molecule.

The least square fitting of the polynomials to the potential curves was done using a MapleV [27] worksheet in each case. From the coefficients R_e,k_e,a,b of the fitted polynomial

$$U(x) = U_e + \frac{k_e}{2}(x-R_e)^2 - a(x-R_e)^3 + b(x-R_e)^4 + c(x-R_e)^5 \tag{15}$$

the spectroscopic constants were calculated in the following way [28], chapter 1.4

$$\omega_e = \frac{1}{2\pi c}\sqrt{\frac{k_e}{\mu}} \tag{16}$$

$$B_e = \frac{\hbar}{4\pi c \mu R_e^2} \tag{17}$$

$$\alpha_e = 24\frac{a(B_e R_e)^3}{\omega_e^3} - 6\frac{B_e^2}{\omega_e} \tag{18}$$

$$\omega_e x_e = \frac{30 B_e^3 R_e^6 a^2}{\omega_e^4} - \frac{6 B_e^2 R_e^4 b}{\omega_e^2} \tag{19}$$

$$D_e = \frac{4B_e^3}{\omega_e^2} \tag{20}$$

In the case of a polynom fit of third degree we set $b = 0$ and $c = 0$.

3 Results and Discussion

3.1 Single-point Calculations

Using the methods described in Section 2, single-point calculations were done for various diatomic systems in the vicinity of the equilibrium geometry using basis sets of varying sizes. In the table below we compare the relative quality of full core and frozen core results with the validity of criterion (6) averaged over the different basis sets. For each molecule except Hydrogen we

3.2 Potential Energy Surfaces and Spectroscopical Parameters

In Figures 2, 3, 4, and 5, the potential energy surface of LiH is shown as computed with different basis sets. For each basis set, MP4, F4, [2/2], Π2 and CCSD(T) results are presented. In this particular example, the Π2 methods is closest to the CCSD(T) result up to $R \approx 5$ bohr where the criterion (6) is satisfied. For larger distances R, this is no longer the case, and in the case of Figures 2 and 4, some unphysical behavior of the Π2 surface is seen in this region where however the criterion (6) indicates that the perturbative results are not acceptable. Comparing the figures, it is also observed that in this case, adding polarization functions slightly enlarges the region where the criterion is satisfied, while adding diffuse functions does not have a large effect.

In order to further judge the quality of the method, a Morse potential and polynomials of degree 3 and 5 were fitted to the data as described in Section 2. The results are displayed in Tables 18 to 22 and Figures 6 (LiH), 7 (HF), 8 (HCl) and 9 (N_2). The color code is blue for MP4, red for Π2, and green for CCSD(T) results. Broken lines represent Morse fits, and full lines the polynomial fit of third degree to the data points that are displayed also. It is seen that in the equilibrium region, the Morse fits often are lying below the data although they reproduce the overall shape of the curves nicely. This leads to the assumption that the vibrational parameters will be acceptable for the Morse fit. The third degree polynomial fits are in most cases more accurate in the region of the minimum but differ significantly from the potential curve for bigger distances. Hence, it is expected that they will produce more accurate estimates for the harmonic frequencies but worse values for the other spectroscopic constants which should be calculated using a 5th degree fitting polynomial.

This is indeed the case. In Table 18 we report the results for the harmonic frequencies, the anharmonic correction term obtained from the Morse fit, the values of the resulting fit parameters $\mathbf{D}_e$ and β and experimental data from Refs. [29] and (in parentheses) [30]. The results for the polynomial fits, 8 Parameter for each molecule, are shown in Tables 19 (LiH),20 (HF), 21 (HCl) and 22 (N_2).

In this context, it should be noted that all results are relatively sensitive to the selection of the data points used in the fitting procedure. In the fits, we usually included all points that are compatible with the criterion (6) in case of the Morse potential – beware that not all these data points are displayed in the figures in order to be able to simultaneously display the Morse and polynomial fits with sufficient resolution –, and 8 points around the minimum for the polynomial fit. The selection of the latter points is plain from the corresponding figures.

In the case of N_2, the MP4 values for $R > 2.6$ bohr were unphysical and excluded from the fit. Also, the criterion (6) was not satisfied in this region. However, since it was observed that the Π2 results agreed rather closely the CCSD(T) results even in this region, we included some points from this region also in order to produce the corresponding Morse fits. The results for the harmonic frequency as obtained from a second Morse fit using only points for which the criterion (6) was satisfied was close to the result displayed in Table 18 while the value for the anharmonicity constant was worse.

The main results using $\Pi 2/6-311G$ and $CCSD(T)/6-311G$ levels of theory are that

- the Π2 results are sufficiently close to the (more expensive) CCSD(T) method using the same fit methodology,
- harmonic frequencies are in most cases better (accuracy 1-3 percent) calculated via polynomial fits of third degree than using Morse fits that can be competitive if these fits of the potential surface are in the equilibrium region of high accuracy, as in the case of the HF molecule, or at least have the same shape as the polynomial fit, as in the case of LiH,
- Morse fits are able to reproduce experimental anharmonic parameter x_e with an accuracy of about 10-30 percent. For this parameter the 5th degree polynomial fit results are of similar accuracy whereas for the remaining three spectroscopic constants the accuracy lies around 5-10 percent.

3.3 Conclusion

In conclusion, the Π2 method is seen to perform similarly to the more expensive CCSD(T) method if the criterion (6) is satisfied. This is equally valid for frozen and full core calculations. Especially for "difficult" molecules like N_2 the quality of the calculated spectroscopic constants can be improved significantly using the Π2 method instead of MP4. For DZ- and DZP-quality basis sets, usually good results are obtained whereas adding diffuse functions does not always yield an improvement for the quality of the perturbational methods.

4 Acknowledgement

Financial support of the *Deutsche Forschungsgemeinschaft* in the project *Die Berechnung der Energiezustände von Quantensystemen mittels effektiver charakteristischer Polynome auf der Grundlage von Störungsreihen* and the *Verein der Freunde der Universität Regensburg e.V.* is gratefully acknowledged. H.H.H. also acknowledges financial support by the *Fonds der Chemischen Industrie*.

5 Tables

For detailed explanations of the meaning of the following data see Sec. 3.1.

Table 1: B_2, R=3.13 bohr, full core

Basis	MP4	F4	[2/2]	Π2	CCSD(T)
3-21G	-48.751134	-48.759092	-48.766450	-48.829253	-48.742630
4-31G	-48.953405	-48.960828	-48.969685	-49.051426	-48.945615
6-31G	-49.013358	-49.021379	-49.029569	-49.106974	-49.583559
6-311G	-49.064917	-49.072378	-49.078850	-49.113003	-49.665516
6-311G(d,p)	-49.113682	-49.120836	-49.127568	-49.156699	-49.102234
6-311G(3df,2p)	-49.152838	-49.158225	-49.164410	-49.184867	-49.139593
6-311++G	-49.066636	-49.074051	-49.080497	-49.114295	-49.670688
Dunning DZ	-49.044619	-49.052475	-49.056773	-49.082403	-49.036684
Dunning DZP	-49.082232	-49.089432	-49.094560	-49.119004	-49.787531
Dunning DZP+diff	-49.083394	-49.090541	-49.095783	-49.120513	-49.786059
Dunning TZ	-49.063643	-49.071194	-49.077818	-49.114272	-49.661605
cc-p-VDZ	-49.072115	-49.080373	-49.087292	-49.126796	-49.727998
cc-p-VTZ	-49.121360	-49.126569	-49.133500	-49.157880	-49.108293
AUG cc-p-VDZ	-49.080497	-49.088505	-49.094912	-49.128833	-49.727220

Table 2: B_2, R=3.13 bohr, frozen core

Basis	MP4	F4	[2/2]	Π2	CCSD(T)
3-21G	-48.748966	-48.757182	-48.764715	-48.839818	-48.740443
4-31G	-48.950762	-48.958444	-48.967563	-49.077452	-48.942960
6-31G	-49.011157	-49.019430	-49.027829	-49.139437	-49.003115
6-311G	-49.030472	-49.037706	-49.046694	-49.158408	-49.600385
6-311G(d,p)	-49.076451	-49.083318	-49.092077	-49.138885	-49.742210
6-311G(3df,2p)	-49.096937	-49.101448	-49.109735	-49.140053	-49.083486
6-311++G	-49.031991	-49.039172	-49.048128	-49.148217	-49.605121
Dunning DZ	-49.017109	-49.024893	-49.030785	-49.073897	-49.009149
Dunning DZP	-49.052655	-49.059479	-49.066122	-49.101248	-49.042690
Dunning DZP+diff	-49.053692	-49.060446	-49.067223	-49.102837	-49.043625
Dunning TZ	-49.033240	-49.040383	-49.049218	-49.139848	-49.609209
cc-p-VDZ	-49.067474	-49.076090	-49.083259	-49.127627	-49.056230
cc-p-VTZ	-49.097514	-49.102643	-49.110571	-49.141289	-49.739408
AUG cc-p-VDZ	-49.072671	-49.081069	-49.087874	-49.127420	-49.713183
AUG cc-p-VTZ	-49.099559	-49.104305	-49.112014	-49.140237	-49.086344

For detailed explanations of the meaning of the following data see Sec. 3.2.

Table 3: BH, R=2.35 bohr, full core

Basis	MP4	F4	[2/2]	Π2	CCSD(T)
3-21G	-25.033956	-25.038944	-25.037724	-25.039643	-25.039020
4-31G	-25.135758	-25.141305	-25.139923	-25.142173	-25.141305
6-31G	-25.167247	-25.172614	-25.171317	-25.173335	-25.172560
6-311G	-25.194634	-25.198815	-25.197736	-25.199589	-25.199549
6-311G(d,p)	-25.233940	-25.237485	-25.236603	-25.237918	-25.238558
6-311G(3df,2p)	-25.251448	-25.254632	-25.253814	-25.255170	-25.256087
6-311++G	-25.195699	-25.199840	-25.198772	-25.200603	-25.200521
Dunning DZ	-25.182810	-25.187302	-25.186184	-25.187947	-25.187667
Dunning DZP	-25.216566	-25.220145	-25.219254	-25.220605	-25.221310

Table 4: BH, R=2.35 bohr, frozen core

Basis	MP4	F4	[2/2]	Π2	CCSD(T)
3-21G	-25.032868	-25.037975	-25.036762	-25.038607	-25.037969
4-31G	-25.134418	-25.140127	-25.138748	-25.140903	-25.140010
6-31G	-25.166151	-25.171634	-25.170355	-25.172270	-25.171502
6-311G	-25.177471	-25.182689	-25.181403	-25.183452	-25.182461
6-311G(d,p)	-25.215910	-25.219945	-25.218987	-25.220360	-25.220584
6-311G(3df,2p)	-25.224928	-25.228724	-25.227752	-25.229357	-25.229595
6-311++G	-25.178434	-25.183602	-25.182326	-25.184360	-25.183330
Dunning DZ	-25.169350	-25.174468	-25.173373	-25.174895	-25.174228
Dunning DZP	-25.202314	-25.206327	-25.205353	-25.206801	-25.207074
Dunning DZP+diff	-25.203131	-25.207155	-25.206173	-25.207645	-25.207926
Dunning TZ	-25.178746	-25.184031	-25.182710	-25.184864	-25.183681
cc-p-VDZ	-25.210964	-25.215117	-25.214243	-25.215388	-25.215654
cc-p-VTZ	-25.226400	-25.230067	-25.229129	-25.230655	-25.231036
AUG cc-p-VDZ	-25.214427	-25.218631	-25.217707	-25.218949	-25.219073
AUG cc-p-VTZ	-25.227304	-25.230885	-25.229966	-25.231497	-25.231938

Table 5: C_2, R=2.38 bohr, full core

Basis	MP4	F4	[2/2]	Π2	CCSD(T)
3-21G	-75.252284	-75.222388	-75.243982	-75.252936	-75.249891
4-31G	-75.566421	-75.535652	-75.557563	-75.566225	-75.563736
6-31G	-75.646444	-75.616554	-75.637781	-75.645915	-75.643978
6-311G	-75.704877	-75.674690	-75.697601	-75.708103	-75.698979
6-311G(d,p)	-75.801671	-75.782256	-75.802303	-75.817771	-75.788482
6-311G(3df,2p)	-75.857046	-75.838547	-75.857945	-75.872142	-75.841211
6-311++G	-75.706746	-75.676529	-75.699533	-75.710187	-75.700551
Dunning DZ	-75.672728	-75.645292	-75.664570	-75.670699	-75.670302
Dunning DZP	-75.768652	-75.751544	-75.768954	-75.781575	-75.759574
Dunning DZP+diff	-75.770327	-75.753102	-75.770683	-75.783539	-75.760971
Dunning TZ	-75.707674	-75.676677	-75.700273	-75.711515	-75.701328
cc-p-VDZ	-75.745753	-75.727009	-75.745961	-75.760684	-75.735719
cc-p-VTZ	-75.828311	-75.808863	-75.828635	-75.843006	-75.813128
AUG cc-p-VDZ	-75.757730	-75.739238	-75.758018	-75.772390	-75.747104
AUG cc-p-VTZ	-75.846440	-75.827665	-75.846836	-75.860367	-75.830932

Table 6: C_2, R=2.38 bohr, frozen core

Table 7: F_2, R=2.82 bohr, full core

Basis	MP4	F4	[2/2]	Π2	CCSD(T)
3-21G	-197.914048	-197.913676	-197.914686	-197.915596	-197.916044
4-31G	-198.741515	-198.740120	-198.741678	-198.742446	-198.742934
6-31G	-198.927632	-198.926179	-198.927784	-198.928565	-198.928941
6-311G	-199.050853	-199.048203	-199.050862	-199.052007	-199.050273
6-311G(d,p)	-199.228720	-199.227931	-199.229618	-199.230985	-199.227379
6-311G(3df,2p)	-199.373606	-199.373260	-199.374940	-199.376634	-199.370768
6-311++G	-199.062715	-199.059467	-199.062705	-199.064118	-199.061342
Dunning DZ	-198.999868	-198.998400	-199.000185	-199.001181	-198.999936
Dunning DZP	-199.135706	-199.135705	-199.136875	-199.138267	-199.134817
Dunning DZP+diff	-199.141913	-199.141836	-199.143180	-199.144732	-199.140587
Dunning TZ	-199.083273	-199.080307	-199.083340	-199.084714	-199.081896
cc-p-VDZ	-199.108729	-199.108744	-199.109637	-199.110683	-199.109431
cc-p-VTZ	-199.332327	-199.331875	-199.333639	-199.335363	-199.329491
AUG cc-p-VDZ	-199.167350	-199.166908	-199.168557	-199.170175	-199.165668

Table 8: F_2, R=2.82 bohr, frozen core

Basis	MP4	F4	[2/2]	Π2	CCSD(T)
3-21G	-197.910679	-197.910373	-197.911371	-197.912322	-197.912688
4-31G	-198.739527	-198.738185	-198.739733	-198.740530	-198.740973
6-31G	-198.925817	-198.924412	-198.926008	-198.926816	-198.927152
6-311G	-199.018279	-199.015239	-199.018143	-199.019307	-199.017749
6-311G(d,p)	-199.186203	-199.185295	-199.187133	-199.188605	-199.184905
6-311G(3df,2p)	-199.302381	-199.301821	-199.303711	-199.305513	-199.299691
6-311++G	-199.029650	-199.025951	-199.029475	-199.030921	-199.028335
Dunning DZ	-198.973694	-198.971942	-198.973893	-198.974882	-198.973803
Dunning DZP	-199.108074	-199.107942	-199.109218	-199.110644	-199.107232
Dunning DZP+diff	-199.114125	-199.113906	-199.115368	-199.116964	-199.112847
Dunning TZ	-199.051797	-199.048433	-199.051705	-199.053087	-199.050471
cc-p-VDZ	-199.101943	-199.102025	-199.102910	-199.104002	-199.102665
cc-p-VTZ	-199.300447	-199.299977	-199.301819	-199.303639	-199.297665
AUG cc-p-VDZ	-199.156386	-199.156002	-199.157664	-199.159352	-199.154747
AUG cc-p-VTZ	-199.323355	-199.322711	-199.324898	-199.327014	-199.319654

Table 9: H_2, R=2.04 bohr

Table 10: HF, R=1.78 bohr, full core

Basis	MP4	F4	[2/2]	Π2	CCSD(T)
3-21G	-99.587341	-99.587377	-99.587455	-99.587567	-99.587855
4-31G	-100.020553	-100.020421	-100.020607	-100.020716	-100.020854
6-31G	-100.116008	-100.115856	-100.116062	-100.116179	-100.116222
6-311G	-100.185280	-100.184699	-100.185271	-100.185487	-100.184984
6-311G(d,p)	-100.300414	-100.300342	-100.300613	-100.300858	-100.299872
6-311G(3df,2p)	-100.350460	-100.350266	-100.350537	-100.350328	-100.348279
6-311++G	-100.197994	-100.196898	-100.197881	-100.198200	-100.196839
Dunning DZ	-100.161709	-100.161429	-100.161830	-100.162077	-100.160993
Dunning DZP	-100.252681	-100.252851	-100.253046	-100.253394	-100.251485
Dunning DZP+diff	-100.259762	-100.259839	-100.260177	-100.260623	-100.257975
Dunning TZ	-100.206147	-100.205273	-100.206083	-100.206361	-100.205299
cc-p-VDZ	-100.233720	-100.233858	-100.233920	-100.234086	-100.233714
cc-p-VTZ	-100.357540	-100.357515	-100.357881	-100.358270	-100.356299
AUG cc-p-VDZ	-100.274331	-100.274283	-100.274685	-100.275104	-100.272813
AUG cc-p-VTZ	-100.376242	-100.376079	-100.376628	-100.377126	-100.374337

Table 11: HF, R=1.78 bohr, frozen core

Basis	MP4	F4	[2/2]	Π2	CCSD(T)
3-21G	-99.585656	-99.585709	-99.585782	-99.585900	-99.586179
4-31G	-100.019559	-100.019443	-100.019623	-100.019737	-100.019876
6-31G	-100.115101	-100.114964	-100.115165	-100.115286	-100.115331
6-311G	-100.168951	-100.168261	-100.168893	-100.169101	-100.168687
6-311G(d,p)	-100.278930	-100.278837	-100.279134	-100.279394	-100.278406
6-311G(3df,2p)	-100.181450	-100.180190	-100.181263	-100.181570	-100.180333
6-311++G	-100.148582	-100.148217	-100.148662	-100.148899	-100.147893
Dunning DZ	-100.238684	-100.238820	-100.239038	-100.239388	-100.237519
Dunning DZP	-100.245697	-100.245729	-100.246099	-100.246551	-100.243944
Dunning DZP+diff	-100.190362	-100.189358	-100.190235	-100.190499	-100.189545
Dunning TZ	-100.230179	-100.230336	-100.230392	-100.230567	-100.230188
cc-p-VDZ	-100.341090	-100.341066	-100.341448	-100.341858	-100.339866
cc-p-VTZ	-100.268763	-100.268738	-100.269140	-100.269578	-100.267275
AUG cc-p-VDZ	-100.354794	-100.354615	-100.355202	-100.355734	-100.352904

Table 13: N_2, R=2.13 bohr, frozen core

Basis	MP4	F4	[2/2]	Π2	CCSD(T)
3-21G	-108.539562	-108.532665	-108.536796	-108.536721	-108.533900
4-31G	-108.997188	-108.989495	-108.993856	-108.993539	-108.991397
6-31G	-109.109713	-109.102202	-109.106410	-109.106049	-109.104272
6-311G	-109.154494	-109.144631	-109.150497	-109.150442	-109.146715
6-311G(d,p)	-109.322322	-109.318754	-109.322942	-109.325404	-109.315396
6-311G(3df,2p)	-109.385107	-109.381840	-109.386001	-109.388636	-109.377395
6-311++G	-109.160368	-109.150046	-109.156203	-109.156178	-109.152568
Dunning DZ	-109.114285	-109.107219	-109.110914	-109.110324	-109.109654
Dunning DZP	-109.282694	-109.280910	-109.283378	-109.285007	-109.278836
Dunning DZP+diff	-109.284769	-109.282916	-109.285467	-109.287150	-109.280793
Dunning TZ	-109.164725	-109.154670	-109.160635	-109.160564	-109.156750
cc-p-VDZ	-109.285651	-109.283574	-109.286444	-109.288372	-109.280947
cc-p-VTZ	-109.382702	-109.379691	-109.383690	-109.386330	-109.375274
AUG cc-p-VDZ	-109.305764	-109.303437	-109.306614	-109.308743	-109.300842
AUG cc-p-VTZ	-109.390285	-109.387183	-109.391206	-109.393790	-109.382817

Table 14: NH^{-2}, R=2.26 bohr, full core

Basis	MP4	F4	[2/2]	Π2	CCSD(T)
3-21G	-54.094661	-54.095802	-54.095699	-54.096561	-54.095198
4-31G	-54.424372	-54.425322	-54.425417	-54.426369	-54.424987
6-31G	-54.503657	-54.504512	-54.504661	-54.505593	-54.504360
6-311G	-54.581564	-54.582176	-54.582849	-54.584287	-54.581664
6-311G(d,p)	-54.667773	-54.668900	-54.669206	-54.670530	-54.666815
6-311G(3df,2p)	-54.750317	-54.751686	-54.752224	-54.754053	-54.748655
6-311++G	-54.804586	-54.788613	-54.799966	-54.803229	-54.790746
Dunning DZ	-54.584163	-54.584522	-54.584831	-54.585502	-54.585032
Dunning DZP	-54.664709	-54.665538	-54.665591	-54.666311	-54.664858
Dunning DZP+diff	-54.888852	-54.873205	-54.884435	-54.887291	-54.871283
Dunning TZ	-54.671265	-54.669518	-54.671746	-54.673220	-54.670152
cc-p-VDZ	-54.586494	-54.587810	-54.587682	-54.588595	-54.586592
cc-p-VTZ	-54.765870	-54.766318	-54.767268	-54.768828	-54.763518
AUG cc-p-VDZ	-54.889913	-54.877445	-54.886912	-54.889656	-54.874069
AUG cc-p-VTZ	-54.975771	-54.954630	-54.970141	-54.974704	-54.947889

Table 15: NH^{-2}, R=2.26 bohr, frozen core

Table 16: OH^-, R=1.90 bohr,full core

Basis	MP4	F4	[2/2]	Π2	CCSD(T)
3-21G	-74.986563	-74.986903	-74.986961	-74.987295	-74.987071
4-31G	-75.361069	-75.361087	-75.361296	-75.361547	-75.361707
6-31G	-75.443624	-75.443595	-75.443829	-75.444074	-75.444262
6-311G	-75.505957	-75.505524	-75.506218	-75.506703	-75.505969
6-311G(d,p)	-75.607961	-75.608074	-75.608423	-75.608907	-75.607340
6-311G(3df,2p)	-75.681392	-75.681588	-75.682087	-75.682812	-75.679964
6-311++G	-75.573757	-75.569762	-75.573085	-75.574151	-75.569692
Dunning DZ	-75.497506	-75.497261	-75.497622	-75.497847	-75.497832
Dunning DZP	-75.591268	-75.591479	-75.591588	-75.591864	-75.591277
Dunning DZP+diff	-75.642081	-75.640607	-75.642330	-75.643264	-75.637489
Dunning TZ	-75.552847	-75.551119	-75.552698	-75.553266	-75.551570
cc-p-VDZ	-75.541436	-75.541772	-75.541806	-75.542094	-75.541693
cc-p-VTZ	-75.679253	-75.679086	-75.679766	-75.680424	-75.677523
AUG cc-p-VDZ	-75.656880	-75.654733	-75.657126	-75.658382	-75.651265
AUG cc-p-VTZ	-75.737126	-75.734535	-75.737342	-75.738742	-75.730277

Table 17: OH^-, R=1.90 bohr, frozen core

Basis	MP4	F4	[2/2]	Π2	CCSD(T)
3-21G	-74.984941	-74.985306	-74.985357	-74.985703	-74.985455
4-31G	-75.360088	-75.360123	-75.360327	-75.360587	-75.360736
6-31G	-75.442736	-75.442722	-75.442952	-75.443204	-75.443384
6-311G	-75.489228	-75.488658	-75.489441	-75.489933	-75.489270
6-311G(d,p)	-75.587051	-75.587132	-75.587521	-75.588032	-75.586460

Table 18: Results of Morse fits of 4 molecules in a 6-311G basis

Molecule	Method	Morse fit				Experimental data [29] ([30])	
		ω_e [cm^{-1}]	$\omega_e x_e$ [cm^{-1}]	$\mathbb{D}_e$ [cm^{-1}]	β [$a.u.$]	ω_e [cm^{-1}]	$\omega_e x_e$ [cm^{-1}]
LiH	MP4	1471	25.60	21091	0.6130	–	–
	Π2	1422	30.01	16833	0.6632	(1405.6)	(23.20)
	CCSD(T)	1418	29.35	17145	0.6555		
N_2	MP4	1859	18.96	45541	1.486	2359.6	14.46
	Π2	2171	12.80	92706	1.216	(2358.6)	(14.32)
	CCSD(T)	2154	16.37	70934	1.379		
HF	MP4	4158	121.3	35642	1.389	4138.5	90.07
	Π2	4145	122.5	35050	1.396	(4138.3)	(89.88)
	CCSD(T)	4133	89.13	34567	1.402		
HCl	MP4	2787	64.09	30353	1.020	2989.7	52.05
	Π2	2731	63.62	29277	1.018	(2990.9)	(52.82)
	CCSD(T)	2737	64.59	28970	1.026		

Table 19: Results of polynomial fits for LiH ($\mu = 0.881$ amu, 6-311G basis)

Parameter	3rd degree Polynomial Fit			5th degree Polynomial Fit			Experimental data [30]
	MP4	Π2	CCSD(T)	MP4	Π2	CCSD(T)	
$U_e[a.u.]$	-8.0183	-8.0194	-8.0197	-8.0182	-8.0193	-8.0196	—
R_e [Å]	1.6232	1.6280	1.6290	1.6229	1.6280	1.6293	1.5957
k_e [mdyn/Å]	1.035	1.006	0.998	0.961	0.932	0.924	—
ω_e[cm^{-1}]	1411	1392	1387	1361	1340	1334	1406
B_e[cm^{-1}]	7.257	7.214	7.204	7.260	7.214	7.202	7.5131
α_e[cm^{-1}]	0.181	0.195	0.200	0.215	0.224	0.228	0.213
$\omega_e\, x_e$[cm^{-1}]	44.57	47.38	48.19	22.55	23.83	24.30	23.20
D_e[cm^{-1}]	$7.67{\cdot}10^{-4}$	$7.74{\cdot}10^{-4}$	$7.77{\cdot}10^{-4}$	$8.27{\cdot}10^{-4}$	$8.37{\cdot}10^{-4}$	$8.40{\cdot}10^{-4}$	$8.62{\cdot}10^{-4}$

6 Figures

For detailed explanations of the meaning of the following data see Sec. 2.

Table 20: Results of polynomial fits for HF ($\mu = 0.957$ amu,6-311G basis)

Parameter	3rd degree Polynomial Fit			5th degree Polynomial Fit			Experimental data [30]
	MP4	Π2	CCSD(T)	MP4	Π2	CCSD(T)	
$U_e[a.u.]$	-100.1860	-100.1862	-100.1857	-100.1853	-100.1855	-100.1850	—
R_e [Å]	0.9348	0.9347	0.9347	0.9376	0.9376	0.9376	0.9168
k_e [mdyn/Å]	9.778	9.767	9.755	8.119	8.107	8.097	—
ω_e[cm^{-1}]	4164	4162	4159	3795	3792	3789	4138
B_e[cm^{-1}]	20.150	20.150	20.150	20.025	20.026	20.026	20.956
α_e[cm^{-1}]	0.842	0.845	0.848	0.906	0.911	0.914	0.798
$\omega_e\, x_e$[cm^{-1}]	224.7	225.6	226.4	90.58	91.49	92.35	89.88
D_e[cm^{-1}]	$18.87{\cdot}10^{-4}$	$18.90{\cdot}10^{-4}$	$18.92{\cdot}10^{-4}$	$22.31{\cdot}10^{-4}$	$22.35{\cdot}10^{-4}$	$22.37{\cdot}10^{-4}$	$21.51{\cdot}10^{-4}$

Table 21: Results of polynomial fits for HCl ($\mu = 0.980$ amu, 6-311G basis)

Parameter	3rd degree Polynomial Fit			5th degree Polynomial Fit			Experimental data [30]
	MP4	Π2	CCSD(T)	MP4	Π2	CCSD(T)	
$U_e[a.u.]$	-460.1804	-460.1818	-460.1813	-460.1796	-460.1806	-460.1806	—
R_e [Å]	1.3315	1.3388	1.3333	1.3369	1.3385	1.3391	1.2746
k_e [mdyn/Å]	4.780	4.753	4.709	3.945	3.872	3.877	—
$\omega_e[\mathrm{cm}^{-1}]$	2879	2870	2857	2615	2590	2592	2991
$B_e[\mathrm{cm}^{-1}]$	9.702	9.596	9.676	9.624	9.601	9.592	10.59
$\alpha_e[\mathrm{cm}^{-1}]$	0.266	0.203	0.275	0.266	0.288	0.272	0.307
$\omega_e\, x_e[\mathrm{cm}^{-1}]$	101.1	76.00	104.6	35.48	40.36	36.94	52.82
$D_e[\mathrm{cm}^{-1}]$	$4.41{\cdot}10^{-4}$	$4.29{\cdot}10^{-4}$	$4.44{\cdot}10^{-4}$	$5.21{\cdot}10^{-4}$	$5.27{\cdot}10^{-4}$	$5.26{\cdot}10^{-4}$	$5.32{\cdot}10^{-4}$

Table 22: Results of polynomial fits for N_2 ($\mu = 7.002$ amu, 6-311G basis)

Parameter	3rd degree Polynomial Fit			5th degree Polynomial Fit			Experimental data [30]
	MP4	Π2	CCSD(T)	MP4	Π2	CCSD(T)	
U_e [a.u.]	-109.1901	-109.1919	-109.1868	-109.1898	-109.1861	-109.1812	—
R_e [Å]	1.1330	1.1355	1.1319	1.1449	1.1328	1.1284	1.0977
k_e [mdyn/Å]	18.69	23.91	24.48	15.54	18.59	19.37	—
$\omega_e[\mathrm{cm}^{-1}]$	2128	2407	2436	1941	2123	2167	2359
$B_e[\mathrm{cm}^{-1}]$	1.875	1.866	1.878	1.836	1.875	1.890	1.998
$\alpha_e[\mathrm{cm}^{-1}]$	0.0333	0.0107	0.0104	0.0248	0.0183	0.0179	0.0173
$\omega_e\, x_e[\mathrm{cm}^{-1}]$	66.93	17.43	17.07	27.11	13.66	13.84	14.32
$D_e[\mathrm{cm}^{-1}]$	$5.82{\cdot}10^{-6}$	$4.49{\cdot}10^{-6}$	$4.47{\cdot}10^{-6}$	$6.57{\cdot}10^{-6}$	$5.86{\cdot}10^{-6}$	$5.75{\cdot}10^{-6}$	$5.76{\cdot}10^{-6}$

For detailed explanations of the meaning of the following data see Sec. 3.2.

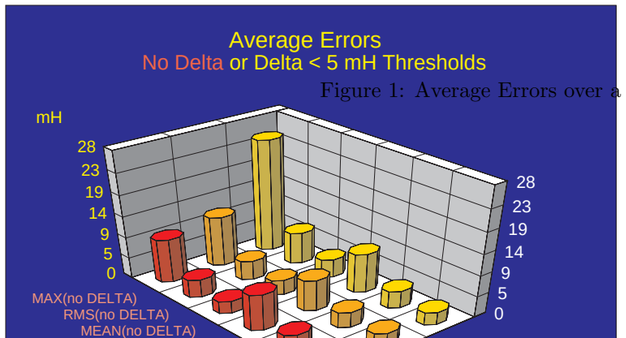

Figure 1: Average Errors over a larger ensemble of molecules (no DELTA) and a subensemble (DELTA) selected by the criterion $\Delta < 5$ mH (ps-file[5])

References

[1] K. Dietz, C. Schmidt, M. Warken, and B. A. Heß. A comparative study of standard and non-standard mean-field theories for the energy, the first and the second moments of Be and LiH. *J. Phys. B: At. Mol. Opt. Phys.*, 25:1705–1718, 1992.

[2] K. Dietz, C. Schmidt, M. Warken, and B. A. Heß. On the acceleration of convergence of many-body perturbation theory: I General theory. *J. Phys. B*, 26:1885–1896, 1993.

[3] K. Dietz, C. Schmidt, M. Warken, and B. A. Heß. On the acceleration of convergence of many-body perturbation theory: II Benchmark checks for small systems. *J. Phys. B*, 26:1897–1914, 1993.

[4] K. Dietz, C. Schmidt, M. Warken, and B. A. Heß. The acceleration of convergence of many-body perturbation theory: Unlinked-graph shift in Møller-Plesset perturbation theory. *Chem. Phys. Lett.*, 207:281–286, 1993.

[5] K. Dietz, C. Schmidt, M. Warken, and B. A. Heß. Systematic construction of efficient many-body perturbation series. *J. Chem. Phys.*, 100(10):7421–7428, 1994.

[6] K. Dietz, C. Schmidt, M. Warken, and B. A. Heß. Explicit construction of convergent MBPT for the $^1\Delta$ state of C_2 and the H_2 ground state at large bond distance. *Chem. Phys. Lett.*, 220(6):397–404, 1994.

[7] H. H. H. Homeier. *Extrapolationsverfahren für Zahlen-, Vektor- und Matrizenfolgen und ihre Anwendung in der Theoretischen und Physikalischen Chemie.* Habilitation thesis, Universität Regensburg, 1996.

[8] H. H. H. Homeier. Correlation energy estimators based on Møller-Plesset perturbation theory. *J. Mol. Struct. (Theochem)*, 366:161–171, 1996.

[9] H. H. H. Homeier. The size-extensivity of correlation energy estimators based on effective characteristic polynomials. *J. Mol. Struct. (Theochem)*, 419:29–31, 1997. Proceedings of the 3^{rd} Electronic Computational Chemistry Conference.

[10] C. Schmidt, M. Warken, and N. C. Handy. The Feenberg series. An alternative to the Møller-Plesset series. *Chem. Phys. Lett.*, 211(2,3):272–281, 1993.

[11] E. Feenberg. Invariance property of the Brillouin-Wigner perturbation series. *Phys. Rev.*, 103(4):1116–1119, 1956.

[12] P. Goldhammer and E. Feenberg. Refinement of the Brillouin-Wigner perturbation method. *Phys. Rev.*, 101(4):1233–1234, 1956.

[13] G. A. Baker, Jr. The theory and application of the Padé approximant method. *Adv. Theor. Phys.*, 1:1–58, 1965.

[14] G. A. Baker, Jr. and P. Graves-Morris. *Padé approximants. Part I: Basic theory.* Addison-Wesley, Reading, Mass., 1981.

[15] G. A. Baker, Jr. and P. Graves-Morris. *Padé approximants. Part II: Extensions and applications.* Addison-Wesley, Reading, Mass., 1981.

[16] P. Bracken. *Interpolant Polynomials in Quantum Mechanics and Study of the One Dimensional Hubbard Model.* PhD thesis, University of Waterloo, 1994.

[17] P. Bracken and J. Čížek. Construction of interpolant polynomials for approximating eigenvalues of a Hamiltonian which is dependent on a coupling constant. *Phys. Lett. A*, 194:337–342, 1994.

[18] P. Bracken and J. Čížek. Investigation of the $^1E_{2g}^-$ states in cyclic polyenes. *Int. J. Quantum Chem.*, 53:467–471, 1995.

[19] P. Bracken and J. Čížek. Interpolant polynomial technique applied to the PPP Model. I. Asymptotics for excited states of cyclic polyenes in the finite cyclic Hubbard model. *Int. J. Quantum Chem.*, 57:1019–1032, 1996.

[20] J. Čížek and P. Bracken. Interpolant polynomial technique applied to the PPP model. II. Testing the interpolant technique on the Hubbard model. *Int. J. Quantum Chem.*, 57:1033–1048, 1996.

[21] J. Čížek, E. J. Weniger, P. Bracken, and V. Špirko. Effective characteristic polynomials and two-point Padé approximants as summation techniques for the strongly divergent perturbation expansions of the ground state energies of anharmonic oscillators. *Phys. Rev. E*, 53:2925–2939, 1996.

[22] J. W. Downing, J. Michl, J. Čížek, and J. Paldus. Multidimensional interpolation by polynomial roots. *Chem. Phys. Lett.*, 67:377–380, 1979.

[23] M. Takahashi, P. Bracken, J. Čížek, and J. Paldus. Perturbation expansion of the ground state energy for the one-dimensional cyclic Hubbard system in the Hückel limit. *Int. J. Quantum Chem.*, 53:457–466, 1995.

[24] J. A. Pople, M. J. Frisch, G. W. Trucks, H. B. Schlegel, P. M. W. Gill, B. G. Johnson, M. A. Robb, J. R. Cheeseman, T. Keith, G. A. Petersson, J. A. Montgomery, K. Raghavachari, M. A. Al-Laham, V. G. Zakrzewski, J. V. Ortiz, J. B. Foresman, C. Y. Peng, P. Y. Ayala, W. Chen, M. Wong, J. Andres, E. Replogle, R. Gomperts, R. L. Martin, D. J. Fox, J. S. Binkley, D. Defrees, J. Baker, J. Stewart, M. Head-Gordon, and C. Gonzalez. *Gaussian 94, Revision B.3.* Gaussian, Inc., Pittsburgh PA, U.S.A., 1995.

[25] In the single point calculations with different basis sets some basis sets were used which are not included in Gaussian 94. These Additional Basis sets (see: EMSL Gaussian Basis Set Order Form) were obtained from the Extensible Computational Chemistry Environment Basis Set Database, Version 1.0, as developed and distributed by the Molecular Science Computing Facility, Environmental and Molecular Sciences Laboratory which is part of the Pacific Northwest Laboratory, P.O. Box 999, Richland, Washington 99352, USA, and funded by the U.S. Department of Energy. The Pacific Northwest Laboratory is a multi-program laboratory operated by Battelle Memorial Institute for the U.S. Department of Energy under contract DE-AC06-76RLO 1830. Contact David Feller, Karen Schuchardt, or Don Jones for further information.

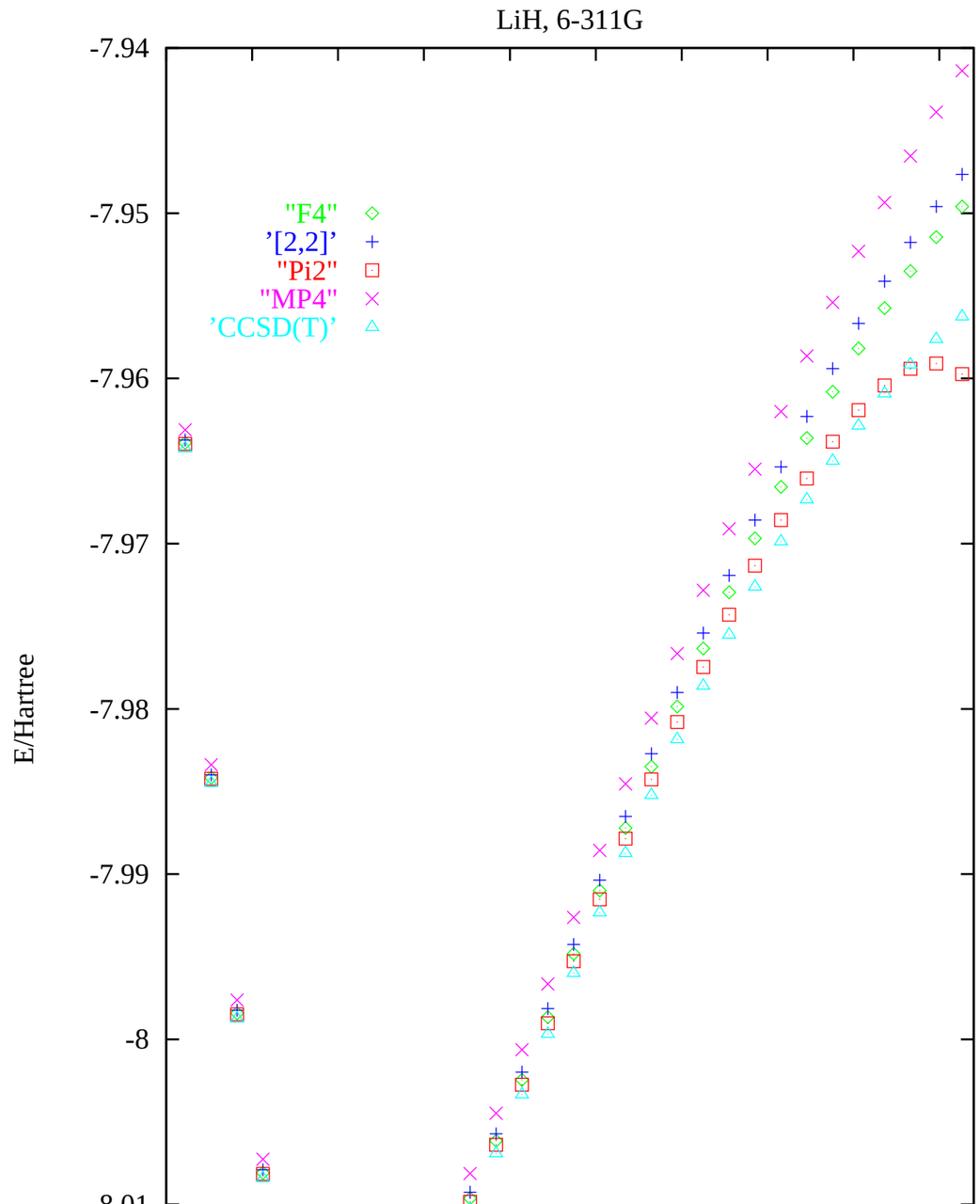
LiH, 6-311G
E/Hartree
-7.94
-7.95
-7.96
-7.97
-7.98
-7.99
-8
-8.01
"F4"
'[2,2]'
"Pi2"
"MP4"
'CCSD(T)'

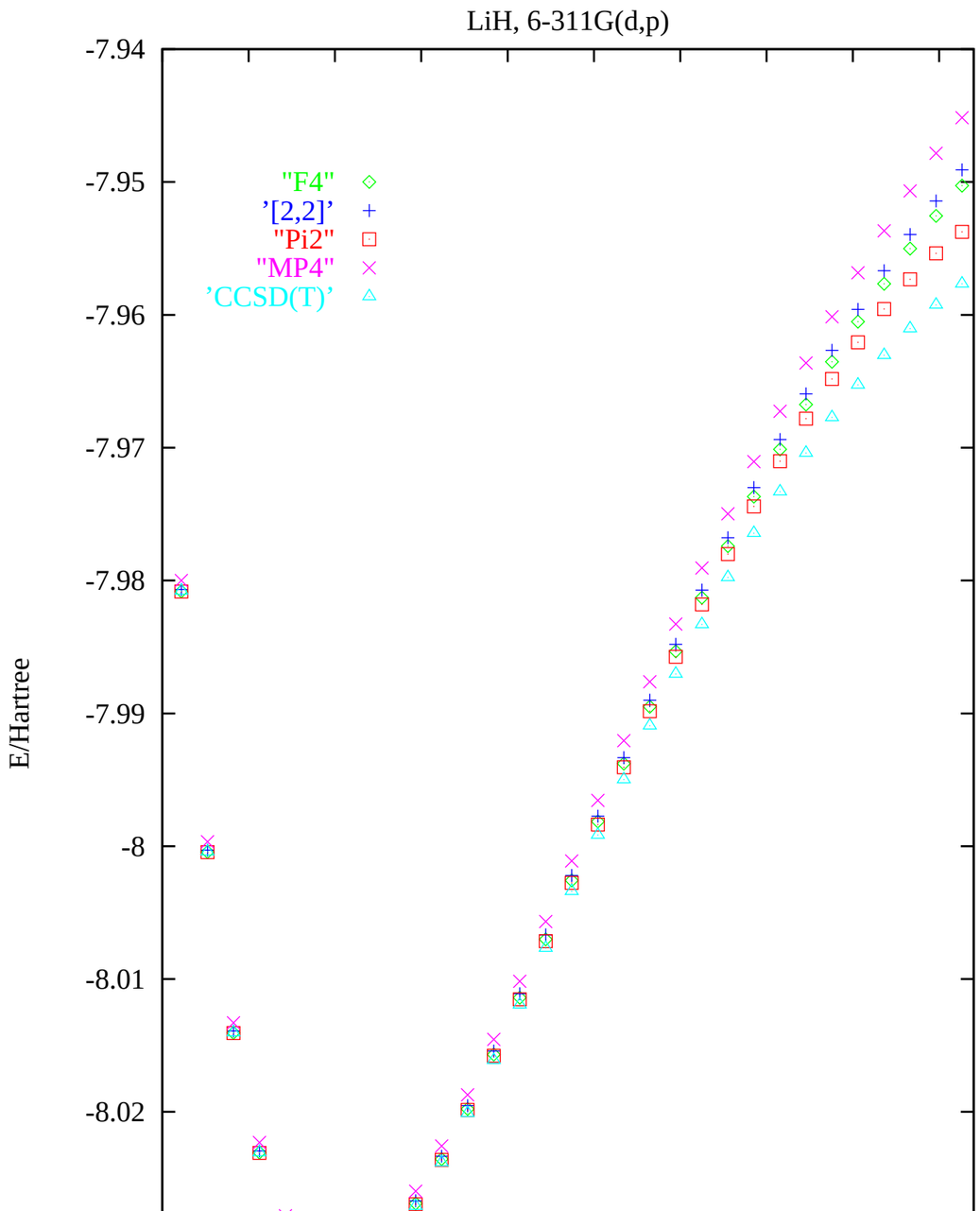
LiH, 6-311G(d,p)
E/Hartree
-7.94
-7.95
-7.96
-7.97
-7.98
-7.99
-8
-8.01
-8.02
"F4"
’[2,2]’
"Pi2"
"MP4"
’CCSD(T)’

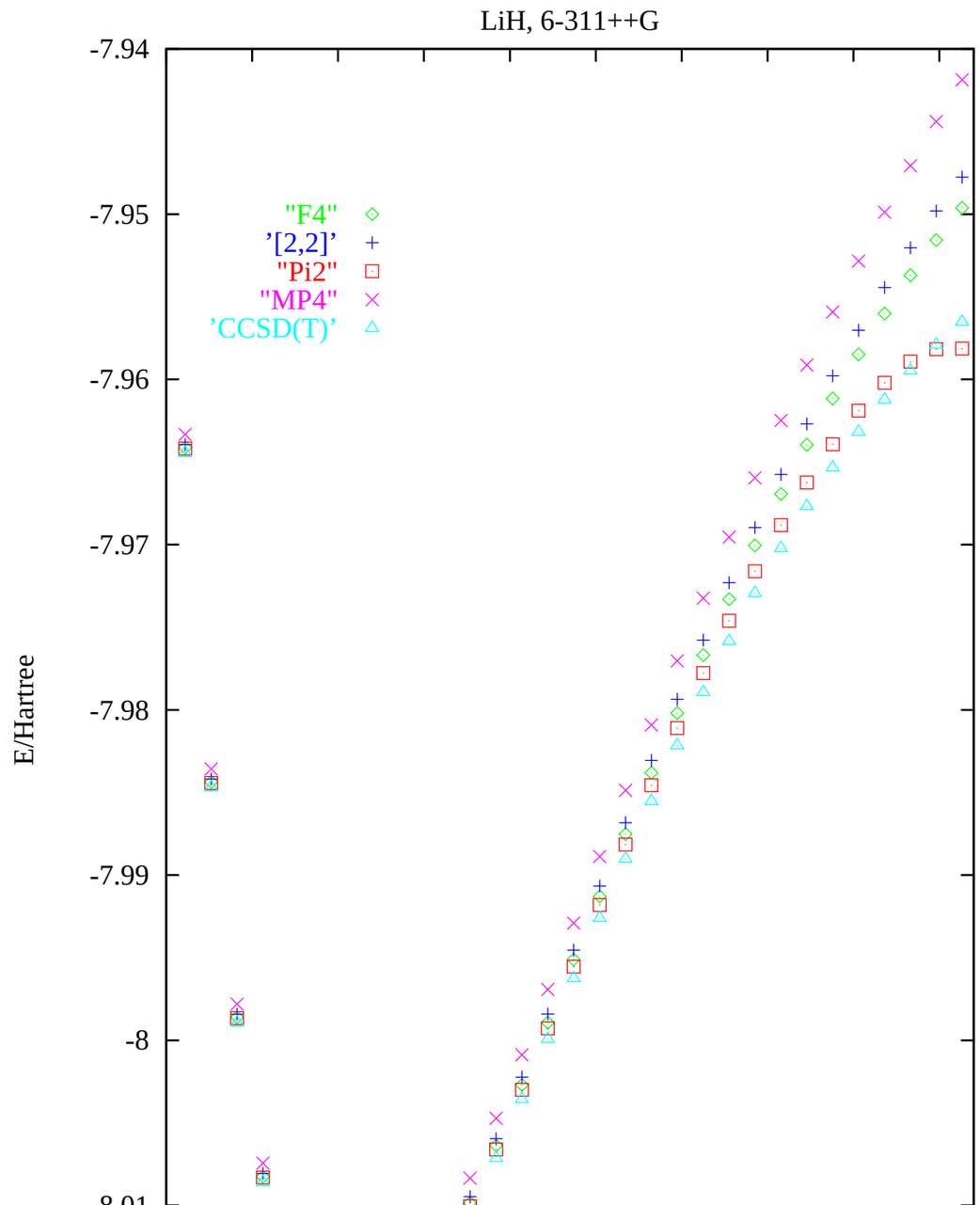
LiH, 6-311++G
E/Hartree
-7.94
-7.95
-7.96
-7.97
-7.98
-7.99
-8
"F4"
'[2,2]'
"Pi2"
"MP4"
'CCSD(T)'

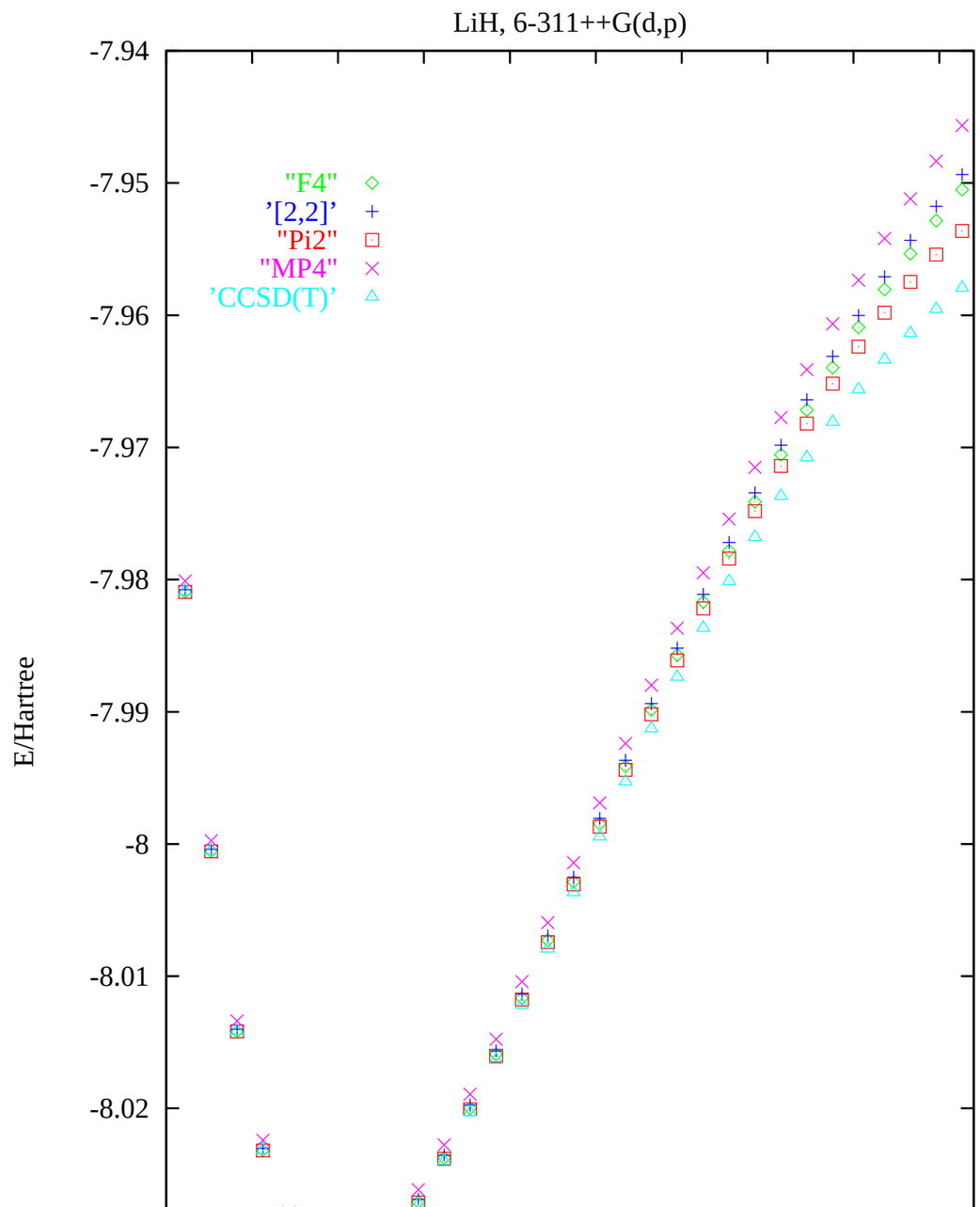
LiH, 6-311++G(d,p)
E/Hartree
-7.94
-7.95
-7.96
-7.97
-7.98
-7.99
-8
-8.01
-8.02
"F4"
’[2,2]’
"Pi2"
"MP4"
’CCSD(T)’

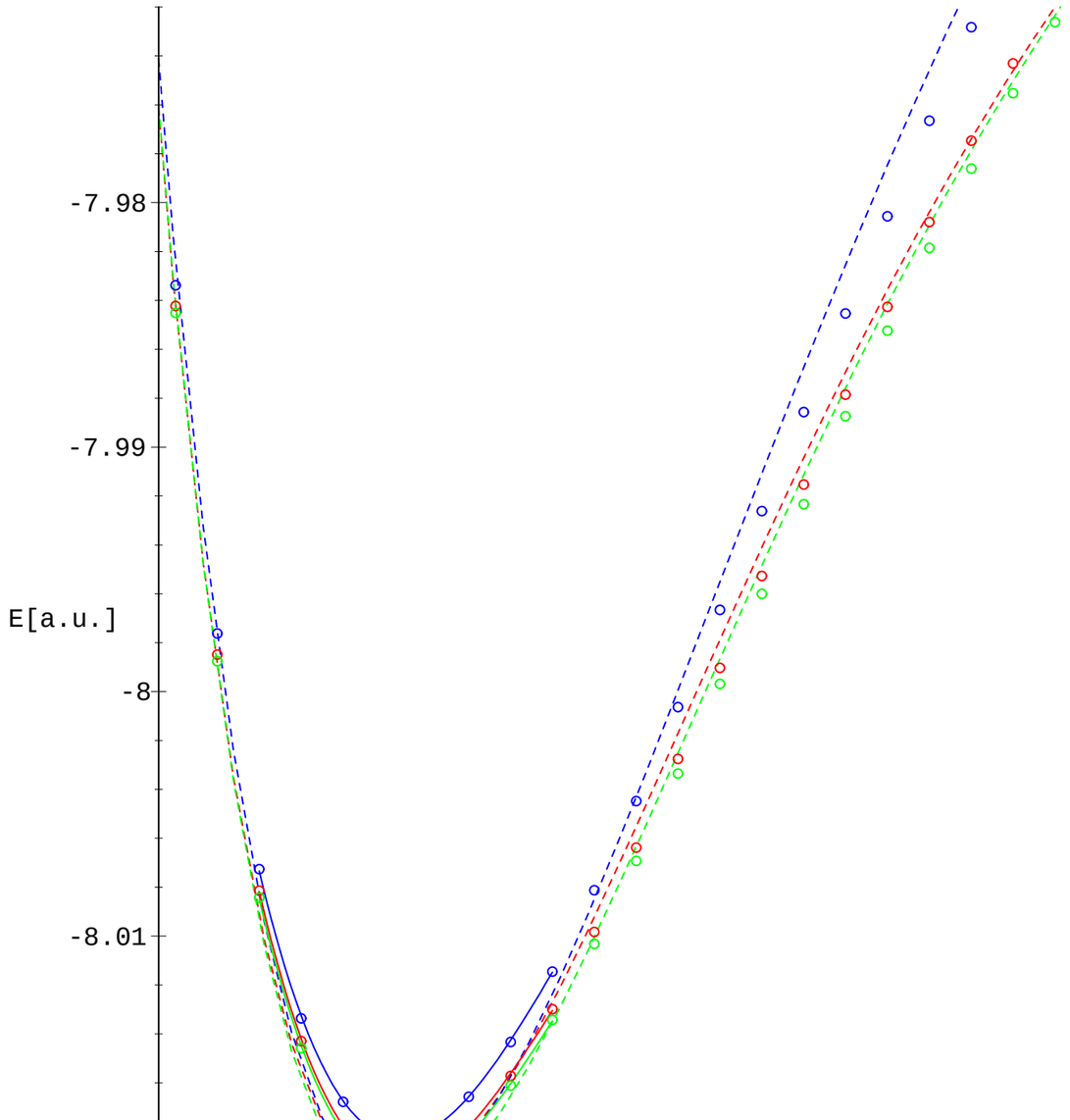
-7.98
-7.99
E[a.u.]
-8
-8.01

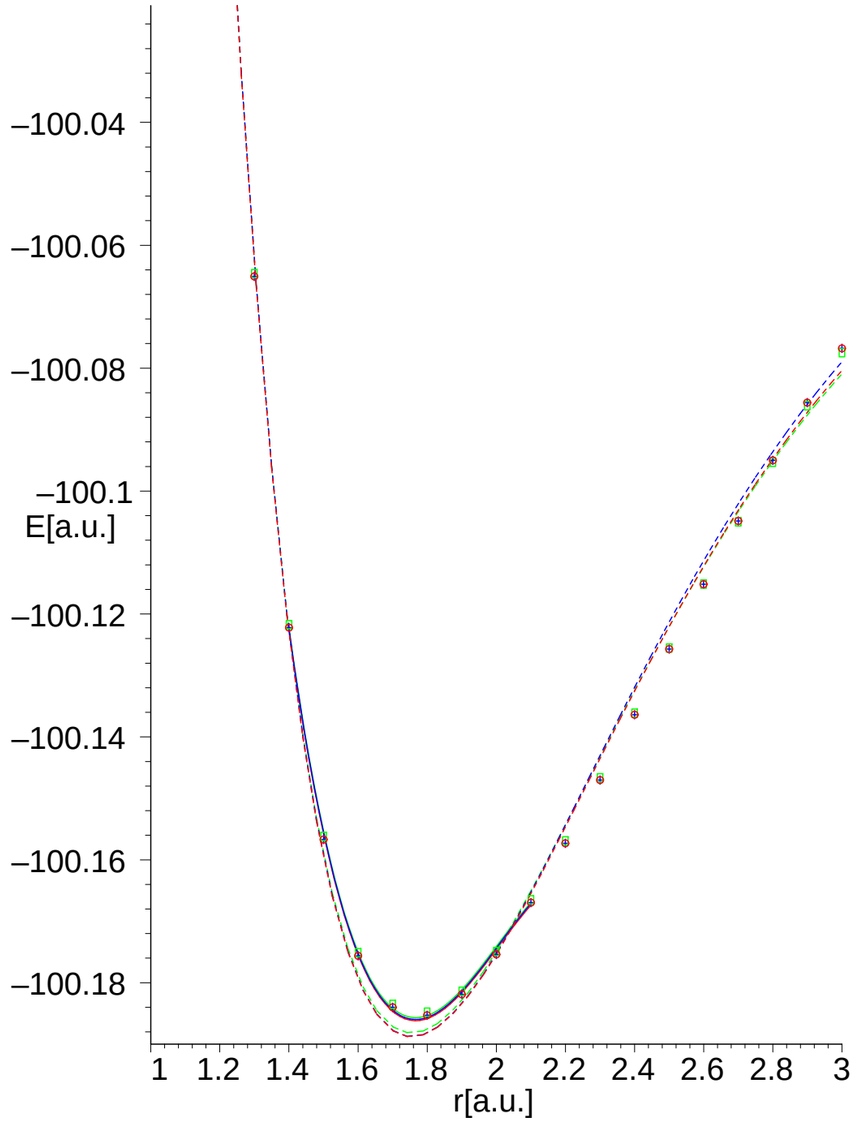

Figure 7: HF: Morse and polynomial fits (ps-file[11])

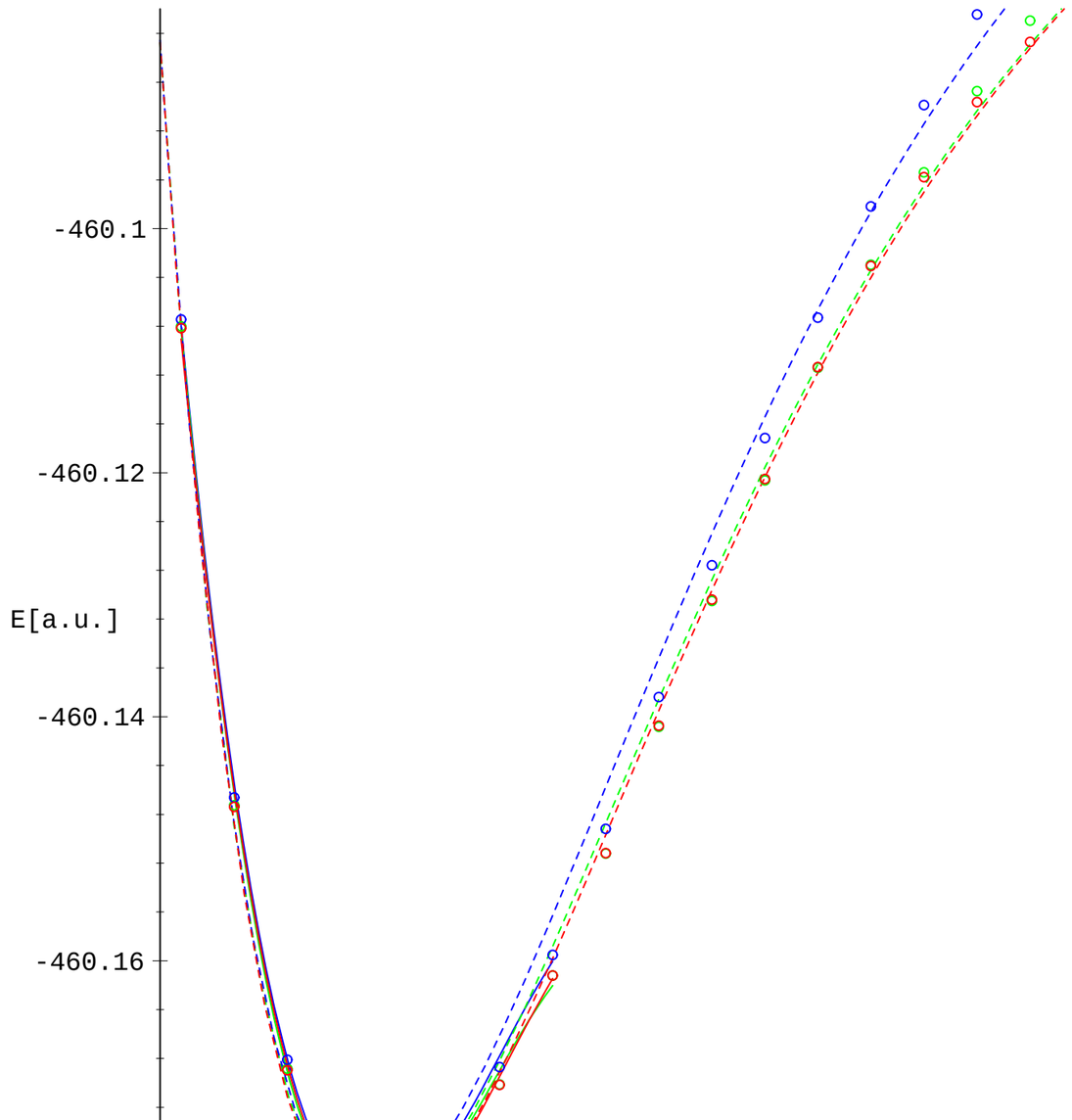
-460.1
-460.12
E[a.u.]
-460.14
-460.16